Exploring the ages of rotating stars using galactic dynamics: a novel approach to calibrating gyrochronology

Ruth Angus, Angus Beane, Adrian Price-Whelan, Elisabeth Newton, Jennifer van Saders, Travis Berger, Jason Curtis, Lauren Anderson, Rocio Kiman

ABSTRACT

The rotational evolution of cool dwarfs is poorly constrained after ~2-3 billion years due to a lack of precise ages and rotation periods for old main-sequence stars. In this work, we use the velocities of low-mass *Kepler* dwarfs to reveal their rotational evolution and demonstrate that kinematics have potential to be a useful tool for calibrating gyrochronology. At ages less than ~1 Gyr we find that a gyrochronology model, calibrated to the Praesepe cluster, accurately predicts the relative ages of stars. At these young ages, lower-mass stars spin more slowly than higher-mass stars because their stronger magnetic fields lead to more efficient angular momentum loss. However, at old ages we find that late G and early K dwarfs rotate *faster* than late K dwarfs of the same age. These results, based on field star rotation periods, align with recent findings from the rotation periods of stars in middle-aged open clusters and theoretical models that vary the rate of surface-to-core angular momentum transport as a function of time and mass. Finally, we find no evidence for mass-dependent heating in a sample of K and M dwarfs in the *Kepler* field.

1. Introduction

1.1. Gyrochronology

It is well established that magnetized stellar winds cause the rotation periods of FGKM dwarfs to increase over time (*e.g.* Schatzman 1962; Weber and Davis 1967; Skumanich 1972; Kawaler 1988; Pinsonneault et al. 1989), and, once fully calibrated, the relationship between period, mass and age can be used to age-date stars via gyrochronology (Barnes 2003, 2007, 2010; Meibom et al. 2011, 2015). However, new photometric rotation periods measured from *Kepler* light curves reveal that rotational evolution is more complicated than previously thought. For example, the M dwarfs in the $\sim$ 700 Myr Praesepe cluster spin more slowly than the G dwarfs – in theory because lower-mass stars have deeper convections zones which generate stronger magnetic fields and more efficient magnetic braking (Schatzman 1962; Weber and Davis 1967). However, in the 1.1 Gyr NGC 6811 cluster, late-K dwarfs rotate at the *same* rate as early-K dwarfs (Curtis et al. 2019). In other words, convection zone depth cannot be the only variable that affects stellar spin-down rate. New semi-empirical models that vary the rate of angular momentum redistribution in the interiors of stars are able to reproduce this flattened period-color relation (Spada and Lanzafame 2019). These models suggest that mass and age-dependent coupling between the cores and envelopes of stars has a significant impact on their surface rotation rates.

Another example of unexpected rotational evolution is seen in old field stars which appear to rotate more rapidly than classical gyrochronology models predict (Angus et al. 2015; van Saders et al. 2016, 2018; Metcalfe and Egeland 2019). A mass-dependent modification to the classical $P_{\mathrm{rot}} \propto t^{\frac{1}{2}}$ spin-down law (Skumanich 1972) is required to reproduce the observations (van Saders et al. 2016, 2018).

The rotational evolution of stars is clearly a complicated process, and to fully calibrate the gyrochronology relations we need reliable ages for large numbers of field stars which span a range of ages. In this paper, we use the velocity dispersions of field stars to gain insight into their rotational evolution.

1.2. Using kinematics as an age proxy

Stars are thought to be born in the thin disk of the Milky Way (MW), orbiting the galaxy with a low out-of-plane, or vertical, velocity (W, or $v_{\mathbf{z}}$), just like the star-forming molecular gas observed in the disk today (*e.g.* Stark and Brand 1989; Stark and Lee 2005; Aumer and Binney 2009; Martig et al. 2014; Aumer et al. 2016). On average, the vertical velocities of stars increase over time (*e.g.* Nordström et al. 2004; Holmberg et al. 2007, 2009; Aumer and Binney 2009; Casagrande et al. 2011). Although the cause of dynamical heating is not well understood, interactions with giant molecular clouds, spiral arms and the galactic bar are thought to play an important role (see Sellwood 2014, for a review of secular evolution in the MW). Although the velocity of any individual star will only provide a weak age constraint, the velocity dispersion of a group of stars can indicate whether, on average, that group is old or young relative to other groups. In this work we compare the velocity dispersions of groups of field stars in the Galactic thin disk to ascertain which groups are older and which younger and draw conclusions based on the implied relative ages.

Vertical velocity, $v_{\mathbf{z}}$, can only be calculated with full 6-dimensional position and velocity information, and unfortunately most stars with measured rotation periods do not have radial velocity (RV) measurements because they are relatively faint *Kepler* targets (∼11th-18th magnitudes). For this reason, we used velocity in the direction of galactic latitude, $v_{\mathbf{b}}$, to approximate $v_{\mathbf{z}}$. The *Kepler* field is positioned at low galactic latitude (b=∼5-20°), so $v_{\mathbf{b}}$ is a close (although imperfect – see section 3) approximation to $v_{\mathbf{z}}$. Because we use $v_{\mathbf{b}}$ rather than $v_{\mathbf{z}}$ we cannot calculate absolute kinematic ages using an age-velocity dispersion relation (AVR). However, regardless of direction, velocity dispersion is expected to monotonically increase over time, and can therefore be used to *rank* groups of stars by age.

This paper is laid out as follows: in section 2 we describe our sample selection process and the methods used to calculated stellar velocities. We also establish that $v_{\mathbf{b}}$ velocity dispersion, $\sigma_{v\mathbf{b}}$, can be used as an age proxy by demonstrating that neither mass-dependent heating nor the selection function seems to strongly affect on our sample. In section 3 we use kinematics to investigate the relationship between rotation period, age and color/$T_{\rm eff}$ in the field and interpret our results in section 4.

2. Method

2.1. The data

We used the publicly available *Kepler*-*Gaia* DR2 crossmatched catalog[1] to combine the McQuillan et al. (2014) catalog of stellar rotation periods, measured from *Kepler* light curves, with the *Gaia* DR2 catalog of parallaxes, proper motions and apparent magnitudes. Reddening and extinction from dust was calculated for each star using the Bayestar dust map implemented in the `dustmaps` *Python* package (M. Green 2018), and `astropy` (Astropy Collaboration et al. 2013). We estimated effective temperatures from dereddened *Gaia* $G_{BP} - G_{RP}$ color, using an 8th-order polynomial relation calibrated using .... stars ask Jason for details.

$$\mathrm{T_{eff}} = 8960 - 4802C + 1931C^2 - 2446C^3 + 2669C^4 - 1324C^5 + 301C^6 - 26C^7, \quad (1)$$

where C is *Gaia* $G_{BP} - G_{RP}$.

Visual binaries and subgiants were removed from the sample by applying cuts to the color-magnitude diagram (CMD), shown in figure 1. A 6th-order polynomial was fit to the main sequence and raised by 0.27 dex to approximate the division between single stars and visual binaries. All stars above this line were removed from the sample. Subgiants were also removed by eliminating stars brighter than 6th magnitude in *Gaia* G-band.

The `Pyia` (Price-Whelan 2018) and `astropy` (Astropy Collaboration et al. 2013; Price-Whelan et al. 2018) *Python* packages were used to calculate stellar velocities. `Pyia` calculates velocity samples from the full *Gaia* uncertainty covariance matrix via Monte Carlo sampling. It therefore not only incorporates uncertainties on the *Gaia* positions parallaxes and proper motions, it also accounts for the *covariance* between these properties. Stars with negative parallaxes, parallax signal-to-noise ratios less than 10, stars fainter than 16th magnitude, stars with absolute $v_{\mathbf{b}}$ uncertainties greater than 1 kms^{-1} and stars with galactic latitudes greater than 15° (justification provided below) were removed from the sample.

2.2. Validating $v_{\mathbf{b}}$ dispersion as an age proxy

There are two main reasons why $v_{\mathbf{b}}$ velocity dispersion may not be a good age proxy. Firstly, mass-dependent heating may act on the sample, meaning that velocity dispersion depends on both age and mass, so cannot be interpreted as a simple age proxy. Secondly,

[1] Available at gaia-kepler.fun

Fig. 1.— Dereddened MS *Kepler* stars with McQuillan et al. (2014) rotation periods on the *Gaia* CMD. We excluded visual binaries by removing stars above the dashed line. Points are colored by their gyrochronal age, according to the Angus et al. (2019) gyrochronology relation. A general age gradient is visible across the main sequence.

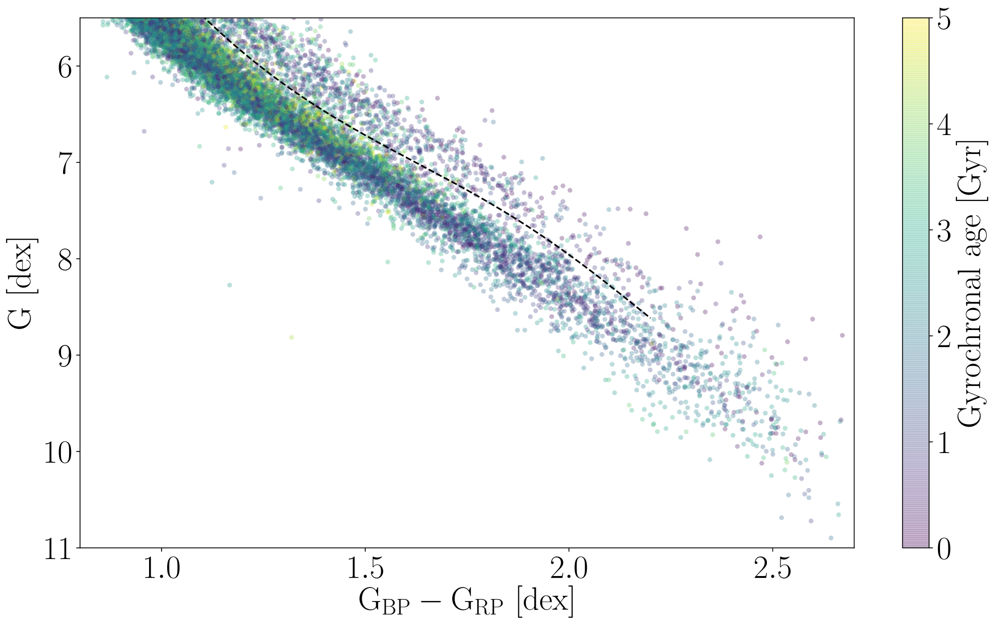

since stars in the *Kepler* field have a range of galactic latitudes, using $v_{\mathbf{b}}$ as a stand-in for $v_{\mathbf{z}}$ may not be equally valid for all stars, introducing a velocity bias for high latitude stars (which are more likely to be cooler and older). In this section we demonstrate that neither of these problems seem to be a significant issue for our data.

If lower-mass stars experience greater velocity changes when gravitationally perturbed and are dynamically heated more efficiently than higher-mass stars, velocity dispersion would be a function of *both* age and mass and cannot be straightforwardly interpreted as an age proxy. So, in order to establish whether $\sigma_{v\mathbf{b}}$ can be used as an age proxy, we searched for signs of mass-dependent heating within the *Kepler* field. Mass-dependent dynamical heating has not been unambiguously observed in the galactic disk because of the strong anti-correlation between stellar mass and stellar age. Less massive stars do indeed have larger velocity dispersions, however they are also older on average. This mass-age degeneracy is highly reduced in M dwarfs because their main-sequence lifetimes are longer than the age of the Universe, however no evidence for mass-dependent heating has been found in M dwarfs (*e.g.* Faherty et al. 2009; Newton et al. 2016).

To investigate whether mass-dependent heating could be acting on the *Kepler* sample, we selected late K and M dwarfs observed by both *Kepler* and *Gaia*, whose MS lifetimes exceed around 11 Gyrs and are therefore representative of the initial mass function. We could not perform this analysis on the McQuillan et al. (2014) sample, because only stars with *detectable* rotation periods are included in it. Since lower-mass stars stay active for longer it is likely that the oldest stars in this sample have low masses. We selected all *Kepler* targets with dereddened *Gaia* $G_{BP} - G_{RP}$ colors greater than 1.2 (corresponding to an effective temperature $\lesssim$ 4800 K) and absolute *Gaia* G-band magnitudes < 4. We also eliminated visual binaries by removing stars above a 6th order polynomial, fit to the MS on the *Gaia* CMD. We then applied the quality cuts described above in section 2.1. To search for evidence of mass-dependent heating we calculated the ($v_{\mathbf{b}}$) velocity dispersion of stars in effective temperature bins. Sigma clipping was performed at the 3σ level to remove high velocity outliers before calculating the standard deviation of stars in each bin. These high velocity outliers may be very old late K and M dwarfs, or they result from using $v_{\mathbf{b}}$ instead of $v_{\mathbf{z}}$, which introduces additional velocity scatter.

Figure 2 shows velocity and velocity dispersion as a function of effective temperature (calculated by transforming dereddened *Gaia* colors using equation 1). Velocity dispersion very slightly *decreases* with decreasing temperature, the opposite of the trend expected for mass-dependent heating, however the slope is only inconsistent with zero at the 1.3 σ level. This trend may be due to a selection bias: cooler stars are fainter and therefore typically closer, with smaller heights above the galactic plane and smaller velocities. The essential point is that we do not find evidence for mass-dependent heating acting on stars in the *Kepler* field, meaning $\sigma_{v\mathbf{b}}$ *can* be used as an age proxy. We also examined the *vertical* velocities of the 537 stars in this sample with RV measurements. Again, we found no evidence for mass-dependent heating: the slope of the velocity dispersion-temperature relation was consistent with zero.

At a galactic latitude of zero, $v_b = v_z$, however for increasing values of b, this equivalence becomes an approximation that grows noisier with b. To test the validity of the $v_{\mathbf{b}}{\sim}v_{\mathbf{z}}$ approximation over a range of latitudes we downloaded stellar data from the *Gaia* Universe Model Snapshot (GUMS) simulation – a simulated *Gaia* catalog (Robin et al. 2012). We downloaded stars from four pointings in the *Kepler* field with galactic latitudes of around 5°, 10°, 15°, and 20°, out to a limiting magnitude of 16 dex. We found that $v_{\mathbf{b}}$ is drawn from a heavy-tailed distribution, centered on $v_{\mathbf{z}}$, with a standard deviation (calculated as 1.5 × the median absolute deviation) that increased with increasing b. The standard deviation of $v_{\mathbf{z}}$-$v_{\mathbf{b}}$ was around 3kms^{-1} at $b \sim 5°$, 4kms^{-}1 at 10°, 6kms^{-}1 at 15°, and 9kms^{-}1 at 20°. Since we are concerned with velocity *dispersions*, rather than velocities themselves, we also compared the $v_{\mathbf{b}}$ and $v_{\mathbf{z}}$ velocity dispersions for stars downloaded from the GUMS simulation. For stars at galactic latitudes of 15° or less, $\sigma_{v\mathbf{b}}$ was consistent with $\sigma_{v\mathbf{z}}$, within uncertainties, however, at higher latitudes the two quantities became significantly different. For this reason we proceeded by only including stars with galactic latitudes less than 15° in our analysis.

Fig. 2.— Top: Stellar velocity ($v_{\mathbf{b}}$) as a function of $T_{\rm eff}$ for *Kepler* K and M dwarfs. Vertical lines indicate different $T_{\rm eff}$-groupings used to calculate velocity dispersion. Pink stars were not included in velocity dispersion calculations as they were either removed as outliers during a sigma clipping process, or they lie at the sparcely populated, extremely cool end of the temperature range. Velocity dispersion and $T_{\rm eff}$ are slightly positively correlated, likely due to a brightness-related selection bias, indicating that mass-dependent heating does not significantly affect low-mass stars in the *Kepler* field.

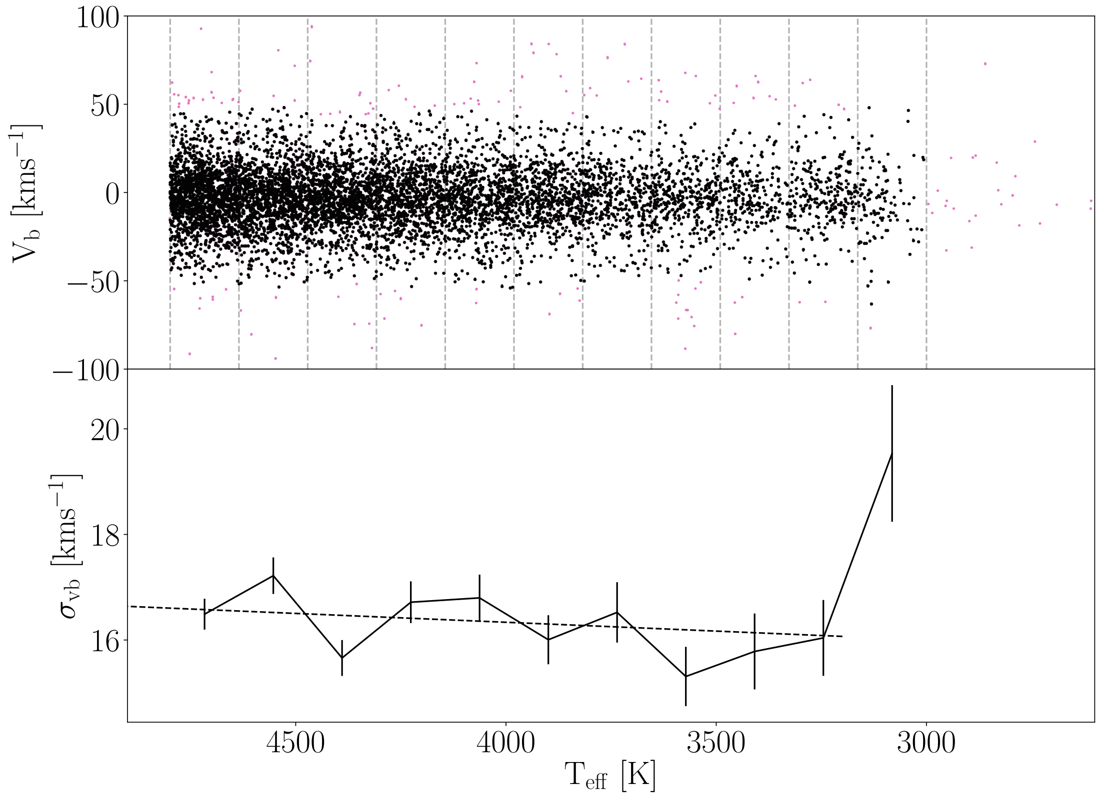

3. Results

3.1. Velocity dispersion of coeval groups

To explore the relationship between rotation period, T_{eff} and age for field K dwarfs, we calculated gyrochronal ages using dereddened *Gaia* photometry (G, G_{BP} and G_{RP}) and rotation periods from McQuillan et al. (2014). We used the Angus et al. (2019) gyrochronology relation which is a simple, separable relation in $G_{BP} - G_{RP}$ color and age, calibrated using the period-color relation of Praesepe and the period-age relation of Praesepe and the Sun. The large number of Praesepe members with precise rotation periods from the *K2* mission (Howell et al. 2014; Douglas et al. 2017; Rebull et al. 2017), spanning spectral types F through early M, makes it a good cluster for calibrating the period-color relation of stars at young ages. However, this is an extremely simple model and although it accurately describes the rotation periods of F and G stars up to around 2.5 Gyr (the age of NGC 6819 – the oldest cluster with available rotation periods), it over-predicts the rotation periods of K dwarfs in the 1.1 Gyr NGC 6811 cluster. These gyrochronal ages are shown on a *Gaia* color-magnitude diagram (CMD) in figure 1. The stars with old gyrochronal ages, plotted in yellow hues, predominantly lie along the upper edge of the MS, where stellar evolution models predict old stars to be, however the majority of these 'old' stars are bluer than $G_{BP} - G_{RP} \sim 1.5$ dex. This suggests that either old M dwarfs are missing from the McQuillan et al. (2014) catalog, or the Angus et al. (2019) gyrochronology relation under-predicts the ages of low-mass stars. Given that lower-mass stars stay active for longer than higher-mass stars (*e.g.* West et al. 2011), and are therefore more likely to have measurable rotation periods at old ages, the latter scenario seems more likely.

To further explore the relationship between rotation period, T_{eff} and age, we first removed high and low velocity outliers by performing 3σ sigma-clipping on the $v_{\mathbf{b}}$ velocities. Without sigma-clipping, we found that a small number of high velocity outliers at the low-temperature end of our sample substantially raised the velocity dispersion for cooler stars. We then selected groups of stars within different gyrochronal age ranges and calculated the standard deviation of $v_{\mathbf{b}}$ velocities ($\sigma_{v\mathbf{b}}$), as a function of effective temperature for each age group. Ages were calculated using dereddened *Gaia* $G_{BP} - G_{RP}$ color, however throughout this paper we show rotation periods as a function of effective temperature, T_{eff}, because it is easier to divide stars into bins of roughly equal numbers in T_{eff}-space than in color-space.

The top panel of figure 3 shows the full McQuillan et al. (2014) sample (excluding visual binaries and subgiants) in grey, with coeval groups (according to the Angus et al. 2019, relation) shown in color. The color of the points corresponds to the age ranges specified in the legend (in Gyr), which also apply to the lines in the lower panel. The bottom panel

Fig. 3.— Top: rotation period vs effective temperature for stars in the McQuillan et al. (2014) catalog. The full catalog, with subgiants and visual binaries removed is shown in grey, and stars selected to be in different age groups (between 3500 and 5500 K) are overlayed in color. These age groups were selected using the Angus et al. (2019) gyrochronology relation. The legend in the center of the figure lists the age range, in Gyr, of each group. Bottom: velocity dispersion vs effective temperature for each age group. The color of the line corresponds to the color of the group shown in the top panel. If the gyrochronal model were correct at all ages, and the stars in each group were the same age across temperatures, the velocity dispersion would be constant as a function of $T_{\rm eff}$. However, the velocity dispersions of the oldest age groups increase with $T_{\rm eff}$, indicating the Angus et al. (2019) gyrochronology model underpredicts the the ages of late-K dwarfs relative to the ages of late G and early K dwarfs at old ages.

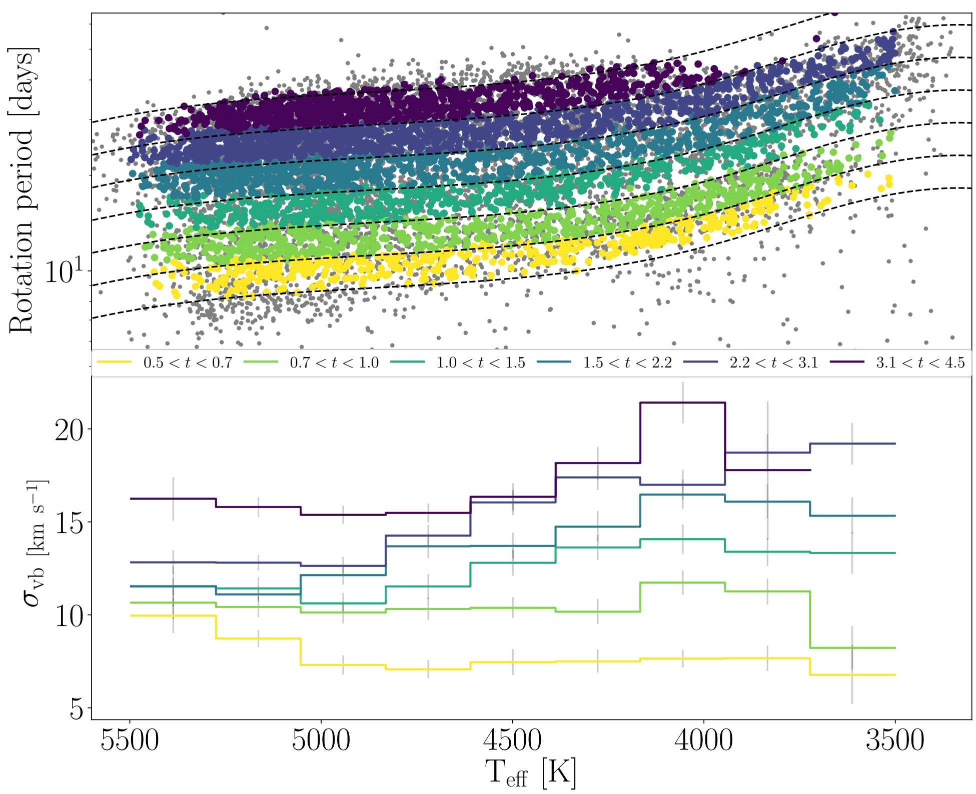

shows the velocity dispersion, $\sigma_{v\mathbf{b}}$ of each age group, as a function of effective temperature. Overall, figure 3 shows that velocity dispersion increases with gyrochronal age across all temperatures, implying that both velocity dispersion and rotation period increases with age as expected. The flat velocity dispersion of young stars as a function of temperature shows that the Praesepe-calibrated gyrochronology relation accurately predicts the relative ages of *young* field stars. If Angus et al. (2019) gyrochronology relation worked at all ages and temperatures, the bottom panel of figure 3 would show a flat relationship between velocity dispersion and T_{eff}at all ages. However, velocity dispersion *increases* as a function of temperature for old stars, meaning the Angus et al. (2019) gyrochronology relation either under-predicts the ages of old, late-K dwarfs, or over-predicts the ages of old early-K and late-G dwarfs[2]. This suggests that the relationship between rotation period and photometric color or T_{eff} flattens out over time, and possibly even inverts.

3.2. The period-T_{eff} relations, revealed

Figure **??** shows rotation period vs. T_{eff} for our sample, coloured by ($v_{\mathbf{b}}$) velocity dispersion, where $\sigma_{v\mathbf{b}}$ was calculated for groups of stars over a grid in $\log_{10}$(period) and temperature. If we assume that mass dependent heating does not strongly affect this sample and $v_{\mathbf{b}}$ at low galactic latitudes is an unbiased tracer of $v_{\mathbf{z}}$, then $v_{\mathbf{b}}$ velocity dispersion can be interpreted as an age proxy and stars plotted in a similar color in figure **??** are similar ages. Interpreted this way, lines of constant age (isochrones) appear to follow the shape of the Praesepe-based gyrochronology model (black solid and dotted lines) at young ages. However, at older ages it appears that the relation between rotation period and T_{eff} flattens out, until eventually rotation period *decreases* with decreasing effective temperature at a given age.

The shape of the period-T_{eff} relations at old ages appears to follow the shape of the upper detection edge. The 'M dwarf dip' (van Saders et al. 2018), a feature of the McQuillan et al. (2014) rotation period catalog characterized by a dearth of slowly rotating M dwarfs between ∼3750 and 4250 K, is reflected in the lines of constant velocity dispersion (and presumed age) in the top panel of figure **??**. If the shape of the upper edge of rotation period measurements is created by a detection limit, it could indicate the rotation periods at which stars of different temperatures become relatively inactive (and their rotation periods therefore become undetectable). If so, figure **??** suggests that stars cooler than ∼4500 K

[2]Since $v_{\mathbf{b}}$ velocity dispersion only provides relative and not absolute ages, it is difficult to tell whether the ages of cool stars are being under-predicted, the ages of hot stars being are over-predicted, or both.

Fig. 4.— Top: Rotation period vs effective temperature for stars in the McQuillan et al. (2014) sample, colored by the velocity dispersions of stars calculated over a grid in $\log_{10}$(period) and $T_{\rm eff}$. Bottom: the velocity dispersions of groups of stars, shown as a solid grid for clarity. The hatched area indicates the temperature regime where selection biases could play an important role, so these velocity dispersions should be interpreted with caution. The black solid lines on both panels show a 1.1 Gyr isochrone, calculated with the Angus et al. (2019) gyrochronology relation, which roughly traces the rotation period gap. The black dashed lines show a 650 Myr isochrone, indicating the location and shape of the Praesepe cluster (to which this gyrochronology model was calibrated). The black points show the 1.1 Gyr NGC 6811 open cluster.

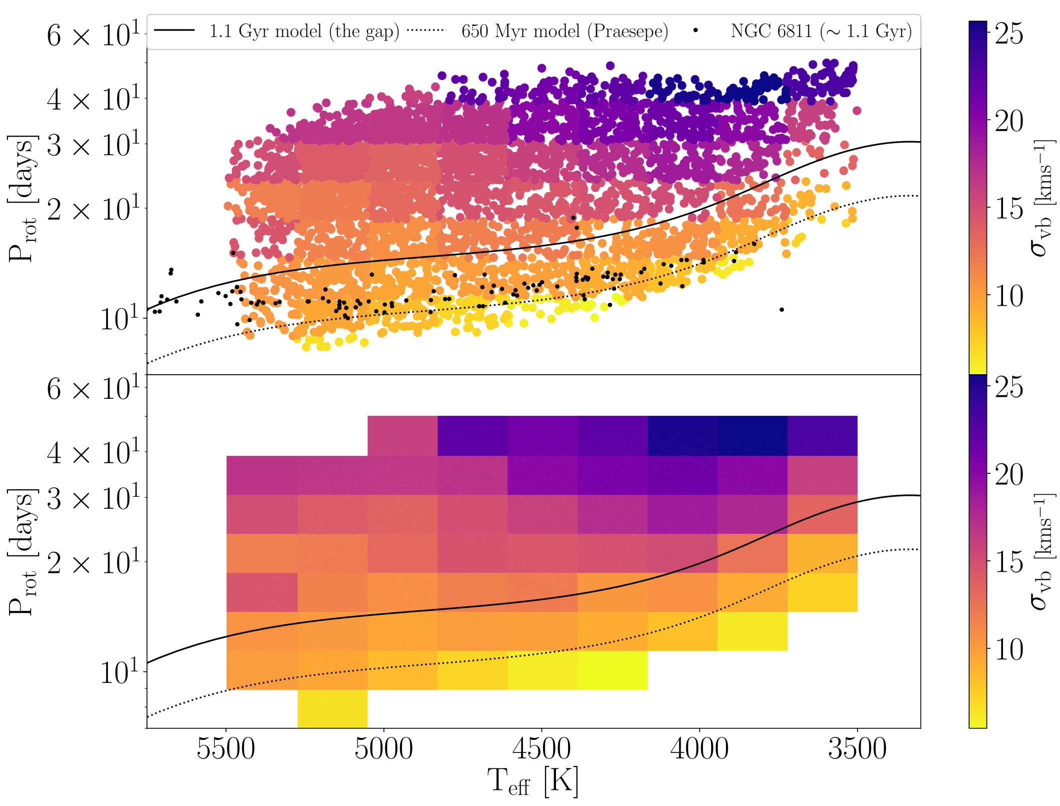

stay active longer than stars hotter than ∼4500 on average.

The velocity dispersions of the coolest stars may be affected by a selection bias – these extremely faint stars are more difficult to detect at larger distances, larger heights above the plane, and therefore larger velocities. It is possible that some high velocity stars of temperatures cooler than ∼4000 K are missing from this sample, and the velocity dispersions may therefore appear lower than they truly are. This could be why the velocity dispersion appears to decrease towards the right of figure **??**.

Fig. 5.— Similar to figure 4, with mass instead of $T_{\rm eff}$ on the x-axis. Masses are from the *Kepler* input catalog. The white lines show the Spada and Lanzafame (2019) rotational evolution models at 0.5, 1, 1.5, 2, 2.5, 4 and 4.57 Gyr, where age increases with rotation period. These models include age and mass-dependent coupling between the stellar core and envelope. The oldest models (4 and 4.57 Gyrs), at the largest rotation periods, show an inversion at ∼0.7-0.5 $M_\odot$, where rotation period briefly decreases with decreasing mass. A similar phenomenon is visible in the velocity dispersions of field stars shown as colored points in the background of this figure.

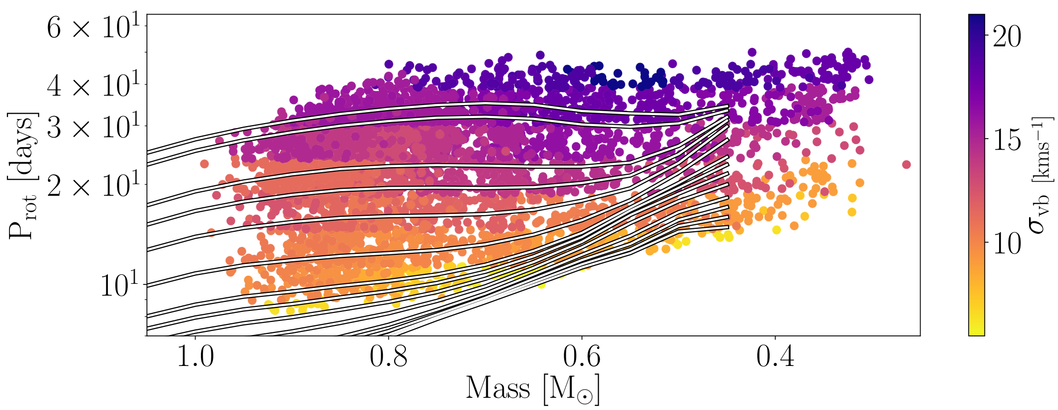

4. Discussion

The results presented above indicate that stars of spectral type ranging from late G to late K follow a braking law that changes over time. These results provide further evidence for 'stalled' rotational evolution of K dwarfs, like that observed in open clusters (Curtis et al. 2019) and reproduced by models that vary angular momentum transport between stellar core and envelope with time and mass (Spada and Lanzafame 2019).

Our results indicate that, at young ages, stellar rotation period decreases with mass. This is probably because lower-mass stars with deeper convection zones have stronger magnetic fields, larger Alfven radii and therefore experience greater angular momentum loss rate. According to the Spada and Lanzafame (2019) models, there is minimal transportation of angular momentum from the surface to the core of the star at these young ages, so the surface slows down but the core keeps spinning rapidly. At intermediate ages, rotation periods appear constant with mass, and at late ages rotation period increases with mass for GK dwarfs. The explanation for this phenomenon, according to the Spada and Lanzafame (2019) models, is that lower-mass stars are still braking more efficiently at these intermediate and old ages but their cores are more tightly coupled with their envelopes, so angular momentum resurfaces and prevents the stellar envelopes from spinning-down rapidly.

The origin of the rotation period gap, first identified by McQuillan et al. (2013) and visible in figures 3 and **??** still remains a mystery. This gap can be seen as an under-density of points between the 0.7-1.0 and 1.0-1.5 Gyr age ranges in figure 3 and roughly follows a line of constant gyrochronal age of around 1.1 Gyr (according to the gyrochronology relation of Angus et al. 2019), as shown in figure **??**. Several explanations for the gap's origin have been proposed, including a discontinuous star formation history (McQuillan et al. 2013; Davenport 2017; Davenport and Covey 2018) and a change in magnetic field structure causing a brief period where rotational variability is reduced and rotation periods cannot be measured (Reinhold et al. 2019). Our results indicate there might be a slight difference in rotational evolution below and above the gap. Stars below the gap appear to be in the regime where wind-braking is dominant (rotation period decreases with increasing mass at a given age) and stars above the gap are in a regime where rotational coupling is dominant (rotation period increases with increasing mass at a given age). This can be seen in figures 3 and 4. For stars below the gap, in the 0.7-1.0 Gyr age range shown in figure 3, velocity dispersion is relatively constant as a function of temperature, however above the gap, in the 1.0-1.5 Gyr age range and older, velocity dispersion increases with $T_{\rm eff}$. In figure 3, velocity dispersion within a given period range appears to *decrease* with decreasing temperature below the gap. The opposite appears to be true above the gap. This suggests that perhaps stars transition from a wind braking regime to a rotational coupling regime as they pass across the gap. However, it is unclear how this process could *create* the gap. A gap could be created if stars rapidly lose angular momentum over a short period of time, leading to a dearth of stars in the gap. However, a sudden redistribution of angular momentum from the core to the surface, should cause stellar rotation periods to *decrease*, not increase. In addition, this theory is not supported by observations of the NGC 6811 cluster whose K dwarf members have already undergone stalled braking below and before they reach the gap. The gap may be associated with a wind braking-rotational coupling transition, however our results only provide weak evidence for this, so we can only speculate until more data become available.

5. Conclusion

We examined the rotational evolution of *Kepler* field stars using their velocity dispersions as a proxy for age. We found that old groups of cool dwarfs selected to be coeval using the Angus et al. (2019) gyrochronology relation do *not* have the same velocity dispersion across all temperatures. This implies that the Angus et al. (2019) relation, which is based on the period-color relation of the 650 Myr Praesepe cluster, does not correctly describe the period-age-color/$T_{\rm eff}$ relation for old stars. It appears that the period-color/$T_{\rm eff}$ relation changes shape over time in a way that qualitatively agrees with theoretical that which include a mass-dependent core-envelope angular momentum transport (Spada and Lanzafame 2019). At young ages, rotation period is anti-correlated with $T_{\rm eff}$: cooler stars spin more slowly than hotter stars of the same age. However, at intermediate ages the relation flattens out and K dwarfs rotate at the same rate, regardless of mass. At old ages, it seems that cooler K dwarfs spin more rapidly than hotter K dwarfs of the same age. We speculate that the rotation period gap (McQuillan et al. 2014) may separate a young regime where stellar rotation periods decrease with increasing mass from an old regime where periods increase with increasing mass, however more data are needed to provide a conclusive result. Finally, when velocity dispersion is interpreted as an age proxy, it appears that the oldest stars in the McQuillan et al. (2014) catalog are cooler than 4500 K, which suggests that lower-mass stars remain active for longer, allowing their rotation periods to be measured at older ages.

This work was partly developed at the 2019 KITP conference 'Better stars, better planets'. Parts of this project are based on ideas explored at the Gaia sprints at the Flatiron Institute in New York City, 2016 and MPIA, Heidelberg, 2017.

This work made use of the gaia-kepler.fun crossmatch database created by Megan Bedell.

Some of the data presented in this paper were obtained from the Mikulski Archive for Space Telescopes (MAST). STScI is operated by the Association of Universities for Research in Astronomy, Inc., under NASA contract NAS5-26555. Support for MAST for non-HST data is provided by the NASA Office of Space Science via grant NNX09AF08G and by other grants and contracts. This paper includes data collected by the Kepler mission. Funding for the *Kepler* mission is provided by the NASA Science Mission directorate.

This work has made use of data from the European Space Agency (ESA) mission *Gaia* (`https://www.cosmos.esa.int/gaia`), processed by the *Gaia* Data Processing and Analysis Consortium (DPAC, `https://www.cosmos.esa.int/web/gaia/dpac/consortium`). Funding for the DPAC has been provided by national institutions, in particular the institutions participating in the *Gaia* Multilateral Agreement.

REFERENCES

R. Angus, S. Aigrain, D. Foreman-Mackey, and A. McQuillan. Calibrating gyrochronology using Kepler asteroseismic targets. *MNRAS*, 450:1787–1798, June 2015. doi: 10.1093/mnras/stv423.

Ruth Angus et al. Towards precise stellar ages: combining isochrone fitting with empirical gyrochronology. *AJ*, 2019.

Astropy Collaboration, T. P. Robitaille, E. J. Tollerud, P. Greenfield, M. Droettboom, E. Bray, T. Aldcroft, M. Davis, A. Ginsburg, A. M. Price-Whelan, W. E. Kerzendorf, A. Conley, N. Crighton, K. Barbary, D. Muna, H. Ferguson, F. Grollier, M. M. Parikh, P. H. Nair, H. M. Unther, C. Deil, J. Woillez, S. Conseil, R. Kramer, J. E. H. Turner, L. Singer, R. Fox, B. A. Weaver, V. Zabalza, Z. I. Edwards, K. Azalee Bostroem, D. J. Burke, A. R. Casey, S. M. Crawford, N. Dencheva, J. Ely, T. Jenness, K. Labrie, P. L. Lim, F. Pierfederici, A. Pontzen, A. Ptak, B. Refsdal, M. Servillat, and O. Streicher. Astropy: A community Python package for astronomy. *A&A*, 558:A33, October 2013. doi: 10.1051/0004-6361/201322068.

M. Aumer and J. J. Binney. Kinematics and history of the solar neighbourhood revisited. *MNRAS*, 397:1286–1301, August 2009. doi: 10.1111/j.1365-2966.2009.15053.x.

Michael Aumer, James Binney, and Ralph Schönrich. Age-velocity dispersion relations and heating histories in disc galaxies. *MNRAS*, 462(2):1697–1713, Oct 2016. doi: 10.1093/mnras/stw1639.

S. A. Barnes. On the Rotational Evolution of Solar- and Late-Type Stars, Its Magnetic Origins, and the Possibility of Stellar Gyrochronology. *ApJ*, 586:464–479, March 2003. doi: 10.1086/367639.

S. A. Barnes. Ages for Illustrative Field Stars Using Gyrochronology: Viability, Limitations, and Errors. *ApJ*, 669:1167–1189, November 2007. doi: 10.1086/519295.

S. A. Barnes. A Simple Nonlinear Model for the Rotation of Main-sequence Cool Stars. I. Introduction, Implications for Gyrochronology, and Color-Period Diagrams. *ApJ*, 722:222–234, October 2010. doi: 10.1088/0004-637X/722/1/222.

L. Casagrande, R. Schönrich, M. Asplund, S. Cassisi, I. Ramírez, J. Meléndez, T. Bensby, and S. Feltzing. New constraints on the chemical evolution of the solar neighbourhood and Galactic disc(s). Improved astrophysical parameters for the Geneva-Copenhagen Survey. *A&A*, 530:A138, Jun 2011. doi: 10.1051/0004-6361/201016276.

J. L. Curtis, M. A. Agüeros, S. T. Douglas, and S. Meibom. A Temporary Epoch of Stalled Spin-Down for Low-Mass Stars: Insights from NGC 6811 with Gaia and Kepler. *arXiv e-prints*, May 2019.

James R. A. Davenport. Rotating Stars from Kepler Observed with Gaia DR1. *ApJ*, 835 (1):16, Jan 2017. doi: 10.3847/1538-4357/835/1/16.

James R. A. Davenport and Kevin R. Covey. Rotating Stars from Kepler Observed with Gaia DR2. *ApJ*, 868(2):151, Dec 2018. doi: 10.3847/1538-4357/aae842.

S. T. Douglas, M. A. Agüeros, K. R. Covey, and A. Kraus. Poking the Beehive from Space: K2 Rotation Periods for Praesepe. *ApJ*, 842:83, June 2017. doi: 10.3847/1538-4357/aa6e52.

Jacqueline K. Faherty, Adam J. Burgasser, Kelle L. Cruz, Michael M. Shara, Frederick M. Walter, and Christopher R. Gelino. The Brown Dwarf Kinematics Project I. Proper Motions and Tangential Velocities for a Large Sample of Late-Type M, L, and T Dwarfs. *AJ*, 137(1):1–18, Jan 2009. doi: 10.1088/0004-6256/137/1/1.

J. Holmberg, B. Nordström, and J. Andersen. The Geneva-Copenhagen survey of the Solar neighbourhood II. New uvby calibrations and rediscussion of stellar ages, the G dwarf problem, age-metallicity diagram, and heating mechanisms of the disk. *A&A*, 475: 519–537, November 2007. doi: 10.1051/0004-6361:20077221.

J. Holmberg, B. Nordström, and J. Andersen. The Geneva-Copenhagen survey of the solar neighbourhood. III. Improved distances, ages, and kinematics. *A&A*, 501:941–947, July 2009. doi: 10.1051/0004-6361/200811191.

Steve B. Howell, Charlie Sobeck, Michael Haas, Martin Still, Thomas Barclay, Fergal Mullally, John Troeltzsch, Suzanne Aigrain, Stephen T. Bryson, Doug Caldwell, William J. Chaplin, William D. Cochran, Daniel Huber, Geoffrey W. Marcy, Andrea Miglio, Joan R. Najita, Marcie Smith, J. D. Twicken, and Jonathan J. Fortney. The K2 Mission: Characterization and Early Results. *PASP*, 126(938):398, Apr 2014. doi: 10.1086/676406.

S. D. Kawaler. Angular momentum loss in low-mass stars. *ApJ*, 333:236–247, October 1988. doi: 10.1086/166740.

Gregory M. Green. dustmaps: A Python interface for maps of interstellar dust. *The Journal of Open Source Software*, 3(26):695, Jun 2018. doi: 10.21105/joss.00695.

Marie Martig, Ivan Minchev, and Chris Flynn. Dissecting simulated disc galaxies - II. The age-velocity relation. *MNRAS*, 443(3):2452–2462, Sep 2014. doi: 10.1093/mnras/stu1322.

A. McQuillan, S. Aigrain, and T. Mazeh. Measuring the rotation period distribution of field M dwarfs with Kepler. *MNRAS*, 432(2):1203–1216, Jun 2013. doi: 10.1093/mnras/stt536.

A. McQuillan, T. Mazeh, and S. Aigrain. Rotation Periods of 34,030 Kepler Main-sequence Stars: The Full Autocorrelation Sample. *ApJS*, 211:24, April 2014. doi: 10.1088/0067-0049/211/2/24.

S. Meibom, S. A. Barnes, D. W. Latham, N. Batalha, W. J. Borucki, D. G. Koch, G. Basri, L. M. Walkowicz, K. A. Janes, J. Jenkins, J. Van Cleve, M. R. Haas, S. T. Bryson, A. K. Dupree, G. Furesz, A. H. Szentgyorgyi, L. A. Buchhave, B. D. Clarke, J. D. Twicken, and E. V. Quintana. The Kepler Cluster Study: Stellar Rotation in NGC 6811. *ApJ*, 733:L9, May 2011. doi: 10.1088/2041-8205/733/1/L9.

S. Meibom, S. A. Barnes, I. Platais, R. L. Gilliland, D. W. Latham, and R. D. Mathieu. A spin-down clock for cool stars from observations of a 2.5-billion-year-old cluster. *Nature*, 517:589–591, January 2015. doi: 10.1038/nature14118.

Travis S. Metcalfe and Ricky Egeland. Understanding the Limitations of Gyrochronology for Old Field Stars. *ApJ*, 871(1):39, Jan 2019. doi: 10.3847/1538-4357/aaf575.

Elisabeth R. Newton, Jonathan Irwin, David Charbonneau, Zachory K. Berta-Thompson, Jason A. Dittmann, and Andrew A. West. The Rotation and Galactic Kinematics of Mid M Dwarfs in the Solar Neighborhood. *ApJ*, 821(2):93, Apr 2016. doi: 10.3847/0004-637X/821/2/93.

B. Nordström, M. Mayor, J. Andersen, J. Holmberg, F. Pont, B. R. Jørgensen, E. H. Olsen, S. Udry, and N. Mowlavi. The Geneva-Copenhagen survey of the Solar neighbourhood. Ages, metallicities, and kinematic properties of 14 000 F and G dwarfs. *A&A*, 418:989–1019, May 2004. doi: 10.1051/0004-6361:20035959.

M. H. Pinsonneault, S. D. Kawaler, S. Sofia, and P. Demarque. Evolutionary models of the rotating sun. *ApJ*, 338:424–452, March 1989. doi: 10.1086/167210.

A. M. Price-Whelan, B. M. Sipőcz, H. M. Günther, P. L. Lim, S. M. Crawford, S. Conseil, D. L. Shupe, M. W. Craig, N. Dencheva, A. Ginsburg, J. T. VanderPlas, L. D. Bradley, D. Pérez-Suárez, M. de Val-Borro, (Primary Paper Contributors, T. L. Aldcroft, K. L.

Cruz, T. P. Robitaille, E. J. Tollerud, (Astropy Coordination Committee, C. Ardelean, T. Babej, Y. P. Bach, M. Bachetti, A. V. Bakanov, S. P. Bamford, G. Barentsen, P. Barmby, A. Baumbach, K. L. Berry, F. Biscani, M. Boquien, K. A. Bostroem, L. G. Bouma, G. B. Brammer, E. M. Bray, H. Breytenbach, H. Buddelmeijer, D. J. Burke, G. Calderone, J. L. Cano Rodríguez, M. Cara, J. V. M. Cardoso, S. Cheedella, Y. Copin, L. Corrales, D. Crichton, D. D'Avella, C. Deil, É. Depagne, J. P. Dietrich, A. Donath, M. Droettboom, N. Earl, T. Erben, S. Fabbro, L. A. Ferreira, T. Finethy, R. T. Fox, L. H. Garrison, S. L. J. Gibbons, D. A. Goldstein, R. Gommers, J. P. Greco, P. Greenfield, A. M. Groener, F. Grollier, A. Hagen, P. Hirst, D. Homeier, A. J. Horton, G. Hosseinzadeh, L. Hu, J. S. Hunkeler, Ž. Ivezić, A. Jain, T. Jenness, G. Kanarek, S. Kendrew, N. S. Kern, W. E. Kerzendorf, A. Khvalko, J. King, D. Kirkby, A. M. Kulkarni, A. Kumar, A. Lee, D. Lenz, S. P. Littlefair, Z. Ma, D. M. Macleod, M. Mastropietro, C. McCully, S. Montagnac, B. M. Morris, M. Mueller, S. J. Mumford, D. Muna, N. A. Murphy, S. Nelson, G. H. Nguyen, J. P. Ninan, M. Nöthe, S. Ogaz, S. Oh, J. K. Parejko, N. Parley, S. Pascual, R. Patil, A. A. Patil, A. L. Plunkett, J. X. Prochaska, T. Rastogi, V. Reddy Janga, J. Sabater, P. Sakurikar, M. Seifert, L. E. Sherbert, H. Sherwood-Taylor, A. Y. Shih, J. Sick, M. T. Silbiger, S. Singanamalla, L. P. Singer, P. H. Sladen, K. A. Sooley, S. Sornarajah, O. Streicher, P. Teuben, S. W. Thomas, G. R. Tremblay, J. E. H. Turner, V. Terrón, M. H. van Kerkwijk, A. de la Vega, L. L. Watkins, B. A. Weaver, J. B. Whitmore, J. Woillez, V. Zabalza, and (Astropy) Contributors. The Astropy Project: Building an Open-science Project and Status of the v2.0 Core Package. *AJ*, 156:123, September 2018. doi: 10.3847/1538-3881/aabc4f.

Adrian Price-Whelan. adrn/pyia: v0.2. Apr 2018. doi: 10.5281/zenodo.1228136.

L. M. Rebull, J. R. Stauffer, L. A. Hillenbrand, A. M. Cody, J. Bouvier, D. R. Soderblom, M. Pinsonneault, and L. Hebb. Rotation of Late-type Stars in Praesepe with K2. *ApJ*, 839:92, April 2017. doi: 10.3847/1538-4357/aa6aa4.

Timo Reinhold, Keaton J. Bell, James Kuszlewicz, Saskia Hekker, and Alexander I. Shapiro. Transition from spot to faculae domination. An alternate explanation for the dearth of intermediate Kepler rotation periods. *A&A*, 621:A21, Jan 2019. doi: 10.1051/0004-6361/201833754.

A. C. Robin, X. Luri, C. Reylé, Y. Isasi, E. Grux, S. Blanco-Cuaresma, F. Arenou, C. Babusiaux, M. Belcheva, R. Drimmel, C. Jordi, A. Krone-Martins, E. Masana, J. C. Mauduit, F. Mignard, N. Mowlavi, B. Rocca-Volmerange, P. Sartoretti, E. Slezak, and A. Sozzetti. Gaia Universe model snapshot. A statistical analysis of the expected contents of the Gaia catalogue. *A&A*, 543:A100, Jul 2012. doi: 10.1051/0004-6361/201118646.

E. Schatzman. A theory of the role of magnetic activity during star formation. *Annales d'Astrophysique*, 25:18, February 1962.

J. A. Sellwood. Secular evolution in disk galaxies. *Reviews of Modern Physics*, 86(1):1–46, Jan 2014. doi: 10.1103/RevModPhys.86.1.

A. Skumanich. Time Scales for CA II Emission Decay, Rotational Braking, and Lithium Depletion. *ApJ*, 171:565, February 1972. doi: 10.1086/151310.

F. Spada and A. C. Lanzafame. On the competing effect of wind braking and interior coupling in the rotational evolution of solar-like stars. *arXiv e-prints*, art. arXiv:1908.00345, Aug 2019.

Antony A. Stark and Jan Brand. Kinematics of Molecular Clouds. II. New Data on Nearby Giant Molecular Clouds. *ApJ*, 339:763, Apr 1989. doi: 10.1086/167334.

Antony A. Stark and Youngung Lee. The Scale Height of Giant Molecular Clouds Is Less than That of Smaller Clouds. *ApJ*, 619(2):L159–L162, Feb 2005. doi: 10.1086/427936.

J. L. van Saders, T. Ceillier, T. S. Metcalfe, V. Silva Aguirre, M. H. Pinsonneault, R. A. García, S. Mathur, and G. R. Davies. Weakened magnetic braking as the origin of anomalously rapid rotation in old field stars. *Nature*, 529:181–184, January 2016. doi: 10.1038/nature16168.

J. L. van Saders, M. H. Pinsonneault, and M. Barbieri. Forward Modeling of the Kepler Stellar Rotation Period Distribution: Interpreting Periods from Mixed and Biased Stellar Populations. *ArXiv e-prints*, March 2018.

E. J. Weber and L. Davis, Jr. The Angular Momentum of the Solar Wind. *ApJ*, 148:217–227, April 1967. doi: 10.1086/149138.

Andrew A. West, Dylan P. Morgan, John J. Bochanski, Jan Marie Andersen, Keaton J. Bell, Adam F. Kowalski, James R. A. Davenport, Suzanne L. Hawley, Sarah J. Schmidt, David Bernat, Eric J. Hilton, Philip Muirhead, Kevin R. Covey, Bárbara Rojas-Ayala, Everett Schlawin, Mary Gooding, Kyle Schluns, Saurav Dhital, J. Sebastian Pineda, and David O. Jones. The Sloan Digital Sky Survey Data Release 7 Spectroscopic M Dwarf Catalog. I. Data. *AJ*, 141(3):97, Mar 2011. doi: 10.1088/0004-6256/141/3/97.

This preprint was prepared with the AAS LaTeX macros v5.0.